Proceeding of the IEEE
International Conference on Robotics and Biomimetics
Dali, China, December 2019

Development of an Adaptive Prosthetic Hand *

Xu Yong[1,2,3], Xiaobei Jing[2,3], Xinyu Wu[1,2]

1. Guangdong Provincial Key Laboratory of Robotics and Intelligent System, Shenzhen Institutes of Advanced Technology, Chinese Academy of Sciences (CAS)
2. CAS Key Laboratory of Human-Machine Intelligence-Synergy Systems, Shenzhen Institutes of Advanced Technology, Chinese Academy of Sciences (CAS)
Shenzhen, Guangdong, 518055, China
{xu.yong, xb.jing, xy.wu}@siat.ac.cn
{yong, jingxiaobei}@hi.mce.uec.ac.jp

Yinlai Jiang[3,4,5], Hiroshi Yokoi[3,4,5]

3. Department of Mechanical Engineering and Intelligent Systems, The University of Electro-communications
4. Center for Neuroscience and Biomedical Engineering, The University of Electro-communications
1-5-1 Chofugaoka, Chofu, Tokyo 182-8585, Japan
5. Beijing Innovation Center for Intelligent Robots and Systems, Beijing 100081, China
jiang.yinlai@uec.ac.jp
yokoi@mce.uec.ac.jp

***Abstract* - Inspired by biomechanics, an adaptive prosthetic hand which not only considered the function of the motion of the digits but also the palm, is presented in this paper. The human hand consists of different kinds of bones, the phalanges in the digits and the metacarpals in the palm, which cooperate to perform adaptable and dexterous motions. Many existent prosthetic hands focus mainly on the movements of the digits, ignoring the palm. The proposed hand has 15 movable joints in the fingers and the thumb, and 2 movable metacarpals in the palm. The thumb and the four fingers are able to flex independently and adaptively wrap along with the shape of the object. The palm could perform an adaptive holding to some extent through the grasping process, due to the movable metacarpals. Furthermore, the hand design is also considered the weight and size limitations for being used as a prosthesis.**

Index Terms – Adaptive, Prosthetic hand.

I. Introduction

Human hands are dexterous to perform various motions and even complex manipulations. A serious impact in both work and daily life will occur to people when they lose their hands due to accidents, diseases or congenital defects. Therefore, as a substitution of the lost hand function, many prosthetic hands have been developed, in which the intuitive control prosthetic hands are highly expected [1]. These prosthetic hands developed so far can be roughly divided into the fully actuated type and underactuated type. The fully actuated prosthetic hands use multiple actuators to achieve high degrees of freedom (DOFs) to realize various hand motions as humans do. Whereas, the fully actuated mechanism with multiple actuator configuration usually brings some issues such as weight increasing, high cost, oversize package, and complex control strategy. In contrast, the underactuated hands that usually contain 1 to 6 actuators [2] have been extensively studied due to the benefits in weight-saving, cost-reducing, human-size package, and control system simplification. Although they could not provide multiple DOFs comparing to the former, there is no lack of feasible and useful design in both experimental tests and practical application. So far, a number of well-designed underactuated hands that introduced the concept of synergy have been developed, and even some have been already commercialized [3-7].

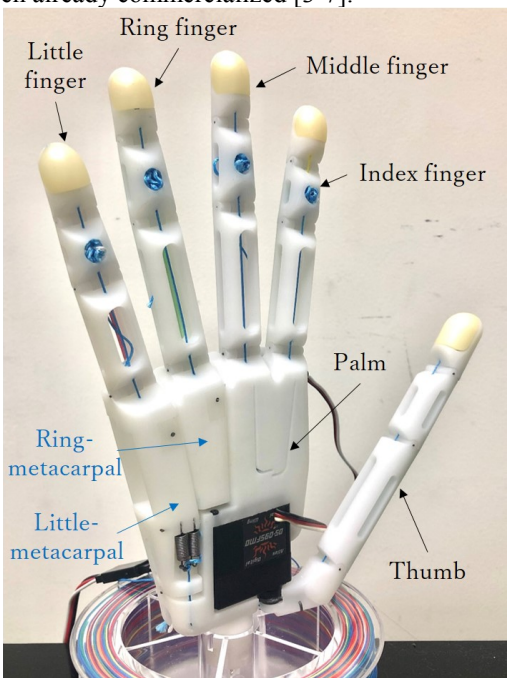

Fig. 1. Designed prosthetic hand

Actually, even though the human hand includes 29 joints, our brain does not control every single joint intentionally, but by utilizing some predefined synergies and coupling interconnections [2, 8-9]. Inspired by biomechanics, a highly biomimetic replica design should have the same kinematic and even dynamic properties of a human hand [10]. However, to naturally replicate both the appearance and complex dexterity of the human hand is always a challenge in this field. The human hand consists of different kinds of bones, the phalanges in the digits and the metacarpals in the palm, which cooperate to perform adaptable and dexterous motions. The existent prosthetic hands mainly focus on the motions of the digits, regarding the palm as a rigid block. Therefore, we will

* This work is partially supported by the JSPS KAKENHI Grant Numbers JP18H03761 and JP19K12877, and a project commissioned by the New Energy and Industrial Technology Development Organization (NEDO), the NSFC-Shenzhen Robotics Research Center Project (U1613219), Shenzhen Institute of Artificial Intelligence and Robotics for Society, the Shenzhen Overseas Innovation and Entrepreneurship Research Program, China (No. KQJSCX20170731164301774).

978-1-7281-6321-5/19//$31.00 ©2019 IEEE

consider releasing DOFs of the phalanges and metacarpals to obtain much more dexterous and anthropomorphic in the hand design. The proposed prosthetic hand is shown in Fig 1. There are 18 movable DOFs in total, 15 movable joints in five digits and 2 movable metacarpals in the palm. Tendon-driven transmissions are adopted in this design owe to the compliance characteristic and compact package. The four fingers are worked as a unit without involving the thumb, which is able to flex adaptively along with the shape of an object. The thumb completely mimics the human hand features of two motion functions, enables them to rotate inward and outward, and also provides adaptive flexion. And the palm can perform an adaptive warp in grasping to some extent.

In this paper, the hand design including the kinematics and static analysis is described in Section II. Section III describes the control method. Section IV shows the results of experiments conducted to validate the hand performance. Finally, section V concludes the study.

II. Hand Design

A. Digits

Each of the four fingers is modeled with the same structure, as shown in Fig. 2. The four fingers are driven by a servo motor with a small size of 29.7×13×33 mm, which is completely embedded in the palm. The same tendon driven mechanism is adapted for every finger, such that, the four fingers are driven by one motor to flex simultaneously as a work unit. Fig. 3 shows the mechanism of the finger. The drive tendon passes through both the PIP and MP joint, with one end fixed on the motor through the driven pulley. When the motor rotates anticlockwise, the drive tendon will be involved up to flex the MP and PIP joints. It is able to provide an adaptive grasp during this process, due to the indeterminacy of this kind of tendon connection. As one driven tendon corresponds to two movable joints, no matter which phalange is blocked due to the contact with an object, the tension force could be transmitted to the other and keep it flexing until totally contacts with the object. Then, the two ends of a passive tendon are fixed on the proximal and distal phalange respectively, crossing through the PIP and DIP joints. The passive tendon will be triggered along with the flexion of the PIP joint, which will involve the DIP joint to flex together with the same angular velocity as the PIP joint, due to this kind of tendon connection can be considered as 1:1 ratio transmission [11]. Therefore, the passive tendon can provide a determinate trajectory for the PIP and DIP joints, which reduces the uncertainty in precision grasping.

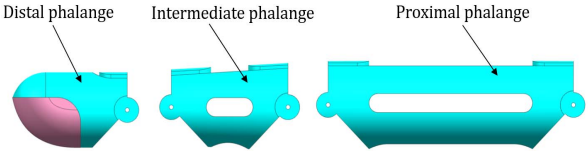

Fig. 2 Structure of the finger.

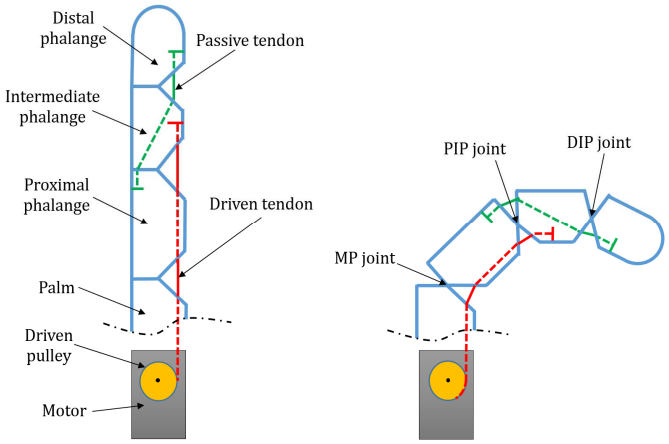

Fig. 3 Tendon-driven mechanism of the finger.

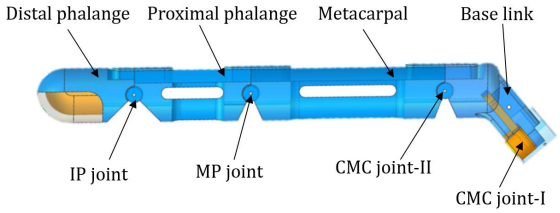

Fig. 4 Structure of the Thumb.

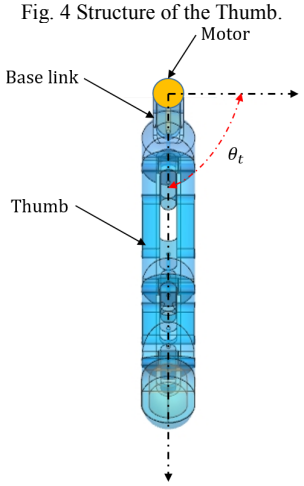

Fig. 5 Adduction/abduction angle range of the thumb.

Two motors are employed for driving the thumb because both the active adduction and adaptive flexion are both play an important role in grasping. Considering the human size package, two smaller servo motor is employed. Both of them are the same types with a size of 31.5×9.5×32.7 mm, which can be embedded in the palm by an overlapping arrangement configuration. The CMC joint is the most special one in the thumb, which is the reason that enables the thumb to obtain two independent DOFs as mentioned. Therefore, the CMC joint has been divided into two parts, one is the CMC-I joint, and the other is the CMC-II joint. The former is connected to one motor through a base link, to drive the whole thumb rotate inward (adduction) and outward (abduction), and the latter is utilized for flexion and extension like other normal finger joints. Fig. 4 shows the structure of the thumb. The CMC-I joint is directly connected with one motor, which can be driven to adduct and abduct with a rotation angle range from 0 ~ 90 degrees (as shown in Fig. 5). The other motor drives the thumb

to flex adaptively through one driven tendon passed through the IP, MP, and CMC-II joint (shown in Fig. 6). Similar to the four fingers, one driven tendon corresponds to three movable joints of the thumb. Such that, the thumb can provide an adaptive wrapping along with the object.

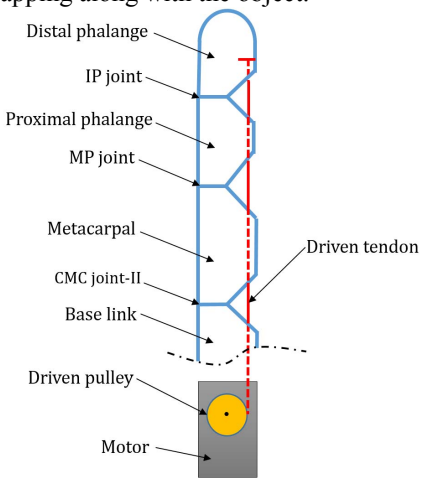

Fig. 6 Tendon-driven mechanism of the thumb.

B. *Palm*

The palm is divided into three-part, one rigid holder shared both of the index and middle finger, and two metacarpals corresponded to the ring and little finger respectively. The motor which drives the thumb to adduct/abduct is also utilized for driving the metacarpals to flex inward. Because the rotation angle range of the thumb is 0 ~ 90 degrees, when θ_t equals to 90 degrees, both of the little-metacarpal and ring-metacarpal flex to the maximum angle as shown in Fig. 7.

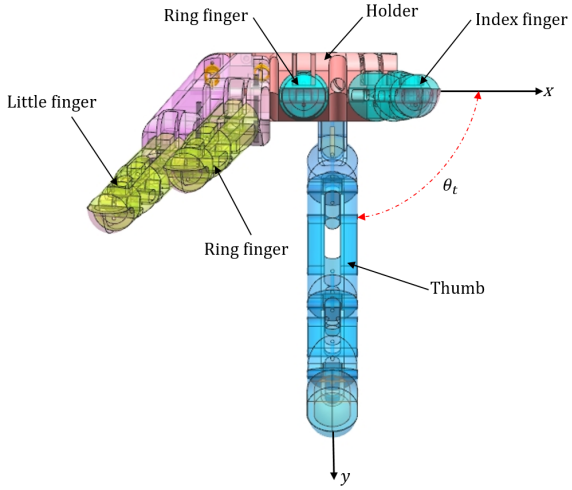

Fig. 7 Complete arch state model.

Taken the CMC-I joint rotation center as ordinate origin, the sketch of the palm is shown in Fig. 8. θ_t is the adduction/abduction rotation angle range of the CMC-I joint θ_2 and θ_3 is the flexion angle of the ring-metacarpal and little-metacarpal respectively, where the angle range of θ_2 is 0 ~ 10 degrees and θ_3 is 0 ~ 15 degrees [12]. θ_4 and θ_5 is the flexion angle of the ring and little finger, the angle range is 0 ~ 90 degrees. θ_1 is the flexion/extension angle of the CMC-II joint, with the range of 0 ~ 50 degrees. In order to mimic the human hand much more naturally, the thumb is designed with some initial angles, such as the fixed angle to the x-y plane between the CMC-I and CMC-II joint is 22 degrees, the initial angle to the same plane between the CMC-II and MP joint is 50 degrees, and the CMC-II joint is fixed with the angle of 45 degrees projected onto the x-y plane.

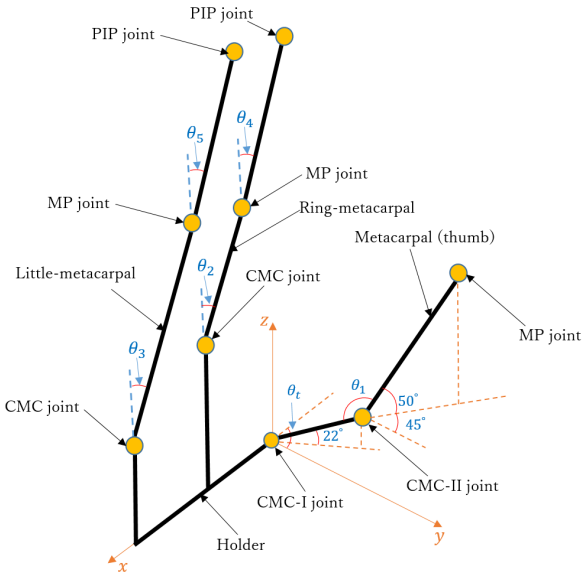

Fig. 8 The sketch of the palm.

The joint trajectories of the metacarpals and fingers are shown in Fig. 9. Firstly, with the CMC-I joint adducts, two of the CMC joints will be involved to flex. And when the CMC-I joint rotates to 90 degrees, the CMC joints will reach to the maximum angles. Then, the CMC-II joint is driven by another motor, which can flex with a range of 0 ~ 50 degrees at any moment in the adduction process. As shown in Fig. 9, the thumb has a curve trajectory, which can provide an inward wrap combining with the metacarpals. Finally, the MP joints are driven by a different motor, which can flex from 0 to 90 degrees. In order to show it clearly, for each MP joint, only plot the whole flex trajectory when the metacarpals reach to their maximum angle.

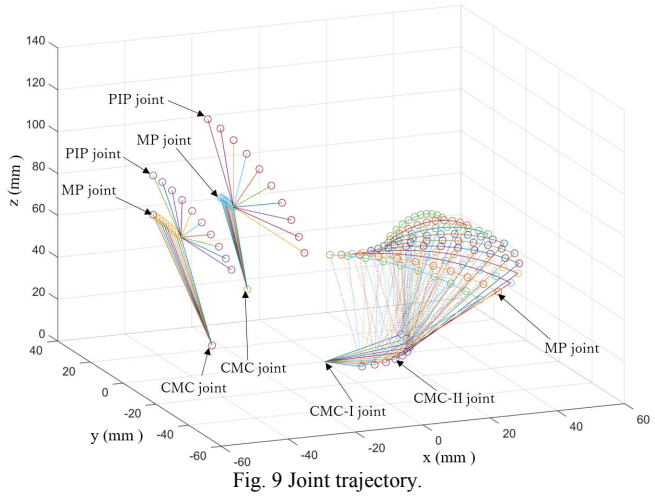

Fig. 9 Joint trajectory.

The added DOFs of the two metacarpals in the palm not only provide much more dexterous of the palm but also increase the movement range of the little and ring finger. If taken the palm as a rigid block again, as shown in Fig. 10. There is no longer any CMC joint in the little-metacarpal and little-metacarpal, such that, they are the fixed part on the holder. The little and ring finger is connected on each of them respectively. And, θ'_2 and θ'_3 is the flexion angle of the ring and little finger, where, the angle range is the same as θ_4 and θ_5, from 0 to 90 degrees. Comparing to the former which has movable metacarpals in the palm, the rigid palm will limit the movement of the ring and little finger.

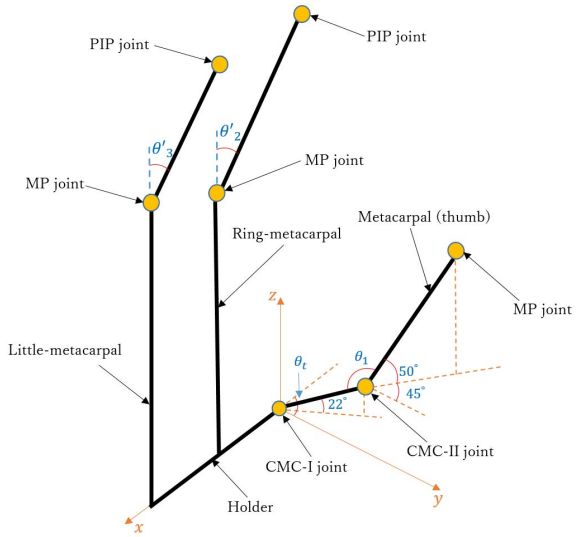

Fig. 10 The sketch of the palm (as a rigid block).

Fig. 11 shows the joint trajectory without the movable little-metacarpal and ring-metacarpal. It's clear that, although the motion range of the thumb remains the same, there are no metacarpals to form a curve wrap with the thumb and the motion range of finger joint is reduced.

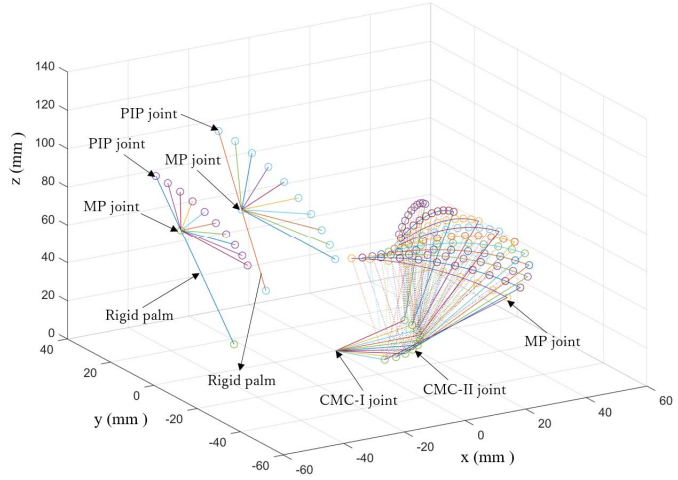

Fig. 11 Joint trajectory (as a rigid palm).

III. Control System

In this study, we use electromyography (EMG) signals to control the prosthetic hand. Preprocessing is as follows. After EMG recording, the controller will run the preprocessing program to extract the feature vector of EMG before the motion control. The EMG is collected by an Amp circuit based on the instrumentation AD620. After signal amplification, the EMG signal is sent to the controller's A/D converter. Firstly, the controller uses signal processing to reduce noise. The A/D converter converts the analog EMG signal into a digital signal with the 2kHz sampling frequency. After A/D conversion, the controller uses a 2nd-order IIR High-pass filter with a cut-off frequency 50Hz to reduce the noise, which caused by body movements. Then converting the discrete data into full-wave rectified data. Secondly, the controller uses the Fast Fourier Transform (FFT) to extract the feature vector from the full-wave rectified data. The data is input into a 128ms epoch where FFT is performed. The result of FFT, the power spectrum of data, is smoothed by moving average whose data window size is 5. Then the power spectrum of frequencies 31Hz, 55Hz, 78Hz, 102Hz, 148Hz, 195Hz, 258Hz, and 320Hz are extracted as feature values. So that the controller can get an 8-dimensional vector from one channel EMG. Finally, as there are three independent channels of EMG, the controller can get a 24-dimensional (24-D) feature vector which combines three 8-dimensional vectors. And these 24-D feature vectors will be used as the teacher-data or input-data of the Artificial Neural Network (ANN).

Furthermore, before controlling the prosthetic hand by EMG, the controller needs to collect enough teacher-data from EMG in different motion patterns of the user. We set that one motion pattern has twenty 24-D feature vectors. Based on the controller's performance, the max number of motion pattern is 5. After the collection of teacher vectors, the controller uses backpropagation to train the ANN. The ANN has 3 layers including an input layer, middle layer, and an output layer. In the input layer, there are 24 neurons because of the 24-D feature vector. In the middle layer, we set the number of neurons as 32. In the output layer, the neurons' number is dependent on the number of motion patterns in teacher vectors collected before. After training, the controller will do pattern recognition by using the ANN. As a result, the ANN will output one result of motion pattern recognition according to one input 24-D vector. Besides, to maintain motion stability. The controller will auto-adjust the result based on the past 10 motions of the prosthetic hand and current result. Finally, the hand will perform the motion.

IV. Experiment

A. *Verified Experiment*

In order to verify the hand deigns, a grasp test had been carried out. In this design, the thumb has two DOFs, the adduction/abduction of CMC-I joint and flexion/extension of the CMC-II joint, driven by two different motors. They are totally independent of each other, whereas, the movement of the CMC-I joint is designed to involve the two metacarpals to flex together. On the other hand, the four fingers are driven through the third motor to ensure that the flexion/extension movement would not be affected by the thumb or the

metacarpals. Fig. 12 shows a grasp test with a sphere object. An assembled prosthetic hand is fixed vertically on the table, then, adjust the hand joints to grasp the object by a motor controller. The grasp posture clearly shows that, when the thumb completely adducted to oppose to the palm, the ring-metacarpals are flexed to their maximum angles. Then, using the motor controller to flex the thumb along with the object. In the whole process, we keep the four fingers on fully extension posture to show that they work as a unit, and could not be affected by the thumb or metacarpals. Therefore, the grasping test verified that the hand-designed is successful and enforceable.

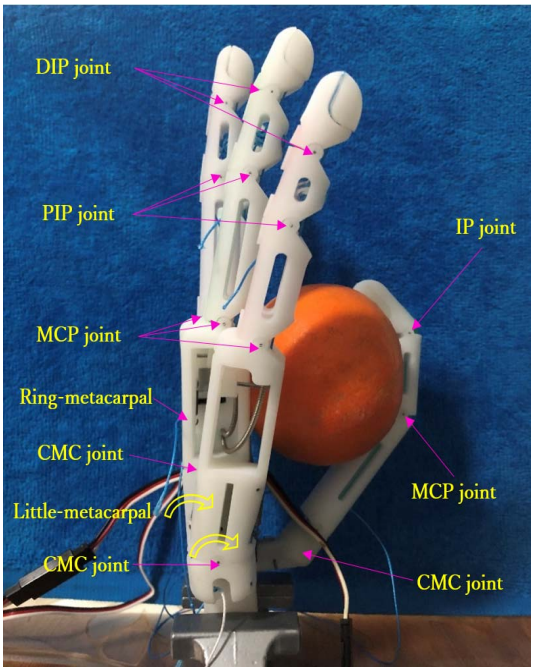

Fig. 12 Grasp test (sphere object).

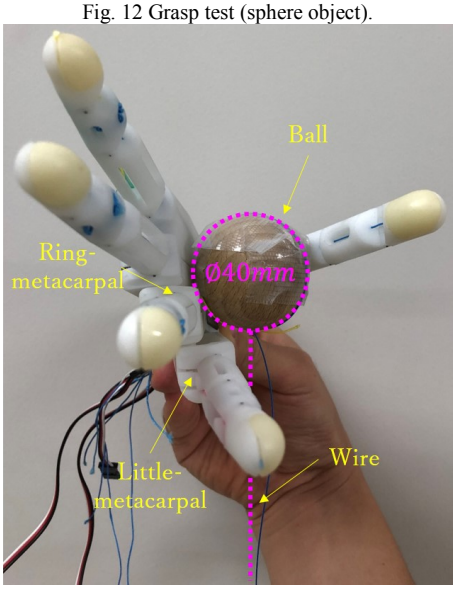

Fig. 13 Load experiment.

Next, a load experiment is conducted to test the holding ability. As shown in Fig. 13, the different load was added vertically onto the wood ball from 0 to 100 g, increased 10 g per turn. For every load, the same holding experiment is carried out ten times. The result is shown in Fig. 14. We can see that, it also most very hard to hold the object when loads over 70 g, however, there are still two successful tasks with 80 g, and one with 70 g.

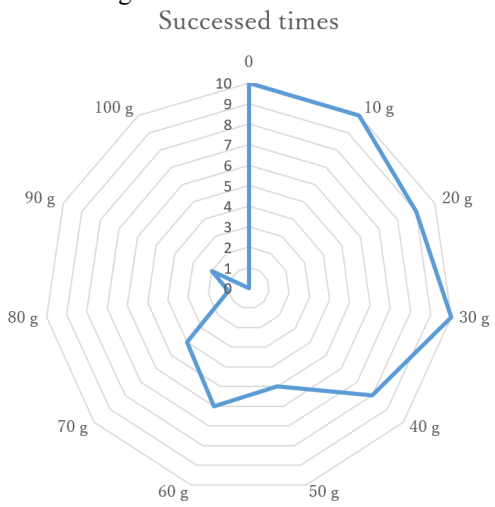

Fig. 14 Result of load experiment.

Finally, we also conducted some motion test experiment for the prosthetic hand to confirm grasp performance. As shown in Fig. 15, the hand can perform various grasp motions, including power grasp, precision grasp, and lateral grasp, with different objects from thin to thick and large to small.

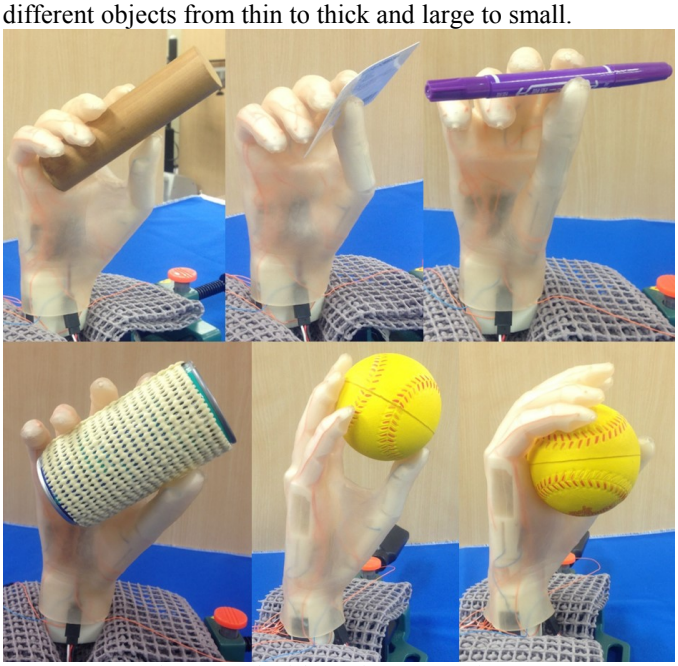

Fig. 15 Result of the motion test experiment.

B. Intuitive Control Test

In this part, the grasp performance of the prosthetic hand (covering with a silicon glove) is verified by the EMG control system. An able-bodied adult male is employed in this experiment, the prosthetic hand is equipped on his right forearm via a socket. The subject was asked to perform several grasp tasks as pick up some objects, place objects to the assigned place, and even a series of consecutive operations. Fig. 16 are a series of images in one task, the images from 1 to

4 show the whole process that the subject picks up a glue stick, then move it to the other marked area, then, remover the can back at last. As seen in Fig. 16, this experiment is successful and could verify the graspability to some extent.

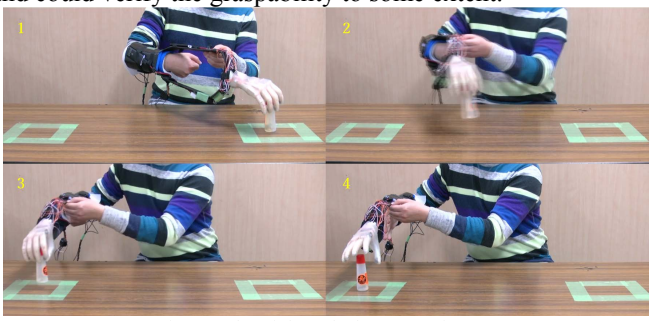

Fig. 16 The pick-and-place experiment.

V. Conclusion

In this study, we proposed a unique prosthetic hand, which is not only able to perform grasp motions but also achieve the arch motion for the palm. The proposed hand has 17 movable joints in total, which is able to mimic the human hand much naturally in both appearance and motions. And, compared to a most conventional prosthetic hand, it proved multi-types of hand motion pattern: power grasp, precision grasp, lateral grasp, and arch function, by using only three motors embedded in the palm. And the prosthetic hand is not only able to form an arch but also passively return to the extension state, like the human hand can adjust the palm to flex or extend between power grasps and spherical grasps.

In addition, the hand design is not only to release hand joints as possible but also consider the weight, cost and size limitations as a prosthesis. The total number of actuators is reduced to three and fully embedded in the palm owe to the novel tendon-driven transmission. Although the prosthetic hand-modeled based on an adult hand size, the whole hand weights about 180 g (include the silicon glove).

However, this prosthesis still has several drawbacks, like the lack of output force and the losing issue of tendons, which will directly relate to the performance of the prosthetic hand. Thus, we will figure out it in future work.

References

[1] J. Kawamura, N. Fukui, M. Nakagawa, T. Fujishita, T. Aoyama and H. Furukawa, "The upper-limb amputees: a survey and trends in kinki area of Japan," The Japanese Association of Rehabilitation Medicine, vol. 36, No. 6, pp. 384-389, 1999.

[2] M. Tavakoli and A. De Almeida, "Adaptive under-actuated anthropomorphic hand: Isr-softhand," The IEEE/RSJ International Conference on Intelligent Robots and Systems (IROS), Sept 2014, pp. 1629–1634.

[3] A.M. Dollar and R.D. Howe, "The Highly Adaptive SDM Hand: Design and Performance Evaluation," Int'l J. Robotics Research, vol. 29, no. 5, pp. 585-597, Feb. 2010.

[4] N. Ulrich and V. Kumar, "Grasping Using Fingers with Coupled Joints," Proc. ASME Mechanisms Conf., 1988.

[5] S. Hirose, "The Development of Soft Gripper for the Versatile Robot Hand," Mechanism and Machine Theory, vol. 13, no. 1, pp. 351-359, 1978.

[6] L. Birglen, C. Gosselin, and T. Laliberte´, "Underactuated Robotic Hands," vol. 40. Springer Verlag, 2008.

[7] M.T. Mason, A. Rodriguez, S.S. Srinivasa, and A.S. Vazquez, "Autonomous Manipulation with a General-Purpose Simple Hand," Int'l J. Robotics Research, vol. 31, no. 5, pp. 688-703, 2011.

[8] T. Feix, "Anthropomorphic hand optimization based on a latent space analysis," Master's thesis, Technische Universitat Wien, October 2011

[9] M. Santello, M. Flanders, and J. F. Soechting, "Postural hand synergies for tool use," The Journal of Neuroscience, vol. 18, no. 23, pp. 10 105–10 115, 1998

[10] Z. Xu and E. Todorov, "Design of a highly biomimetic anthropomorphic robotic hand towards artificial," IEEE International Conference on Robotics and Automation (ICRA), pp. 3458-3492, 2016.

[11] K. Anzawa, H. Sasaki, S. Jeong, and T. Takahashi, "Development of a finger joint mechanism with a low backlash 3D cam," The 2009 JSME Conference on Robotics and Mechatronics, vol. 2A2, no. B09, pp. 1-4, 2009.

[12] A. I. Kapandji, "Physiologie de l'appareil locomoteur 6 edition," MALOINE, 2005.